Kinetics of $Fc_\epsilon RI$ Dimer Formation by Specific Monoclonal Antibodies on Mast Cells†

Reinhard Schweitzer-Stenner,*,‡ Enrique Ortega,§ and Israel Pecht*,‖

Institute of Experimental Physics, Fachbereich 1, University of Bremen, 28359 Bremen, Germany, Instituto de Investigaciones Biomedicas, Universidad Nacional Autonoma de Mexico, Ap. Postat 70288 D.F., CP04510, Mexico, and Department of Chemical Immunology, The Weizmann Institute of Science, Rehovot 76100, Israel

Received January 12, 1994; Revised Manuscript Received May 16, 1994®

ABSTRACT: Clustering of the type I receptor for Fc_ϵ domains constitutes the signal initiation leading to mast cell secretory response. In order to characterize the relationship between the lifetime of clustered Fc_ϵ receptors and the cellular response we have studied the rates of association and dissociation of monoclonal, IgG class antibodies (mAbs) specific for the α-subunit of type 1 receptor for IgE ($Fc_\epsilon RI$) (designated as F4, J17, and H10) to and from this receptor on live rat mucosal-type mast cells (line RBL-2H3) were measured at three different temperatures (25, 15, and 4 °C). These antibodies dimerize the $Fc_\epsilon RI$ on these cells and induce their secretion, thus providing clear evidence that Fc_ϵ receptor dimers are sufficient for the stimulus [Ortega et al. (1988), *EMBO J. 7*, 4101]. Marked differences in the response to the different mAbs have been explained in terms of possible orientational constraints imposed by them on the Fc_ϵ receptor dimers. Interaction kinetics between the Fab fragments of these mAbs and the $Fc_\epsilon RI$ have previously been measured and found to be best fitted by a two-reaction-step model involving a conformational transition from a low-affinity (l) to a high-affinity (h) state of the receptor–ligand complex [Ortega et al. (1991) *Biochemistry 30*, 3473]. Analysis of the interaction kinetics between the corresponding intact mAbs and the $Fc_\epsilon RI$ therefore requires consideration of this $l \rightarrow h$ transition for both complexes involved, namely, the monomeric $Fc_\epsilon RI$–mAb and the dimeric $Fc_\epsilon RI$–mAb–$Fc_\epsilon RI$ complexes. This was done by assuming the involvement of the following $Fc_\epsilon RI$ dimer species: all l- or h-state dimers D_{ll} and D_{hh} and a hybrid D_{lh} with one receptor in the l state and the other in the h state. A self-consistent set of rate constants was derived by fitting the experimental results to this model. At 25 °C the all-h-state dimers D_{hh} turned out to be preferentially stabilized, probably by interaction with other cellular components. Different dimer formation rates were observed for each of the three mAbs, indicating that the dimer distribution among different states is determined by the individual epitope–binding site combination and also by the geometry of the respective complexes. Employing the theoretical model proposed by Dembo et al. (1979, *J. Immunol. 123*, 1864–1872) we correlated the time course of $Fc_\epsilon RI$ dimerization with that of the cell's secretory response to the three mAbs. This suggested that the $Fc_\epsilon RI$ dimers must attain a lifetime longer than a distinct threshold value in order to become effective secretagogues. This condition is met by the species D_{lh} and D_{hh}, whereas D_{ll} decays too fast and hence does not induce the secretory response. Moreover, we suggest that significant desensitization may take place at high $Fc_\epsilon RI$ dimer concentrations. As a consequence H10 and J17 become less effective in causing release than F4 in spite of their larger dimerizing capacity. Results of this and earlier studies using these type 1 Fc_ϵ receptor specific antibodies have clearly suggested that the signaling capacity of these receptors depends on the driving forces leading to their clustering and also on fine tuning provided by both lifetime and structural properties of the produced receptor oligomers.

The primary process initiating the cascade coupling the immunological stimulus of mast cells and basophils to their secretory response is the clustering of IgE class antibodies bound to the type I Fc_ϵ receptor ($Fc_\epsilon RI$)[1] by multivalent antigens [cf. Kinet and Metzger (1990) and the references cited therein]. We aim at resolving the parameters which determine the efficiency of the stimulatory signal of $Fc_\epsilon RI$ clusters. In a theoretical model rationalizing the triggering efficiency of antigen receptor clusters DeLisi (1980) proposed that in addition to the cluster's size a threshold length of its lifetime is one such parameter. A third one is the proximity of adjacent $Fc_\epsilon RI$s within a cluster. The influence of this parameter has been experimentally explored by several groups. McConnell and co-workers (Balakrishnan et al., 1982; Weis et al., 1982) found that mobile univalent, hapten (DNP) derivatized lipids embedded in a lipid monolayer triggered the response of mast cells (RBL-2H3 line) carrying monoclonal, DNP-specific IgE antibodies. This and the effects of the lipids' viscosity led them to conclude that a localized increase in $Fc_\epsilon RI$ concentration is sufficient to trigger release of these cells. These findings thus indicate that triggering efficiency increases with the decrease of distance among $Fc_\epsilon RI$ below a critical threshold value. This notion, however, was challenged by experiments using divalent DNP haptens of different lengths and flexibility as cross-linking reagents for cell-bound, hapten-specific IgE antibodies. All of these ligands

† The research reported here was carried out at the Weizmann Institute of Science, where R.S.-S. was a recipient of a short-term fellowship from the Minerva Foundation, Germany, and E.O. was a graduate student. It was supported in part by grants from the Thyssen Foundation, Germany, and the Corown Endowment Immunological Research at the Weizmann Institute of Science.

‡ University of Bremen.

§ Universidad Nacional Autonoma de Mexico.

‖ The Weizmann Institute of Science.

® Abstract published in *Advance ACS Abstracts,* July 1, 1994.

[1] Abbreviations: RBL-2H3, rat basophilic leukemia cells, subline 2H3; FCS, fetal calf serum; mAb, monoclonal antibody; $Fc_\epsilon RI$, type I receptor for Fc_ϵ domains; AC, association rate curve; DCD, dissociation rate curve observed after sample dilution; DCDI, dissociation rate curve observed after sample dilution with excess unlabeled IgE.

0006-2960/94/0433-8813$04.50/0

were found to be capable of cross-linking IgEs into dimers in solution and on the surface of mast cells (Schweitzer-Stenner et al., 1987, 1992b; Posner et al., 1991). The corresponding $Fc_\epsilon RI$ aggregates, however, differ in terms of their triggering efficiency. While the latter is rather limited for haptens with short spacers (Reck et al., 1985; Erickson et al., 1986; Kane et al., 1986), bivalent haptens with a rigid macromolecular spacer as avidin presumably avoiding direct interactions between receptors were found to be effective secretagogues (Kane et al., 1988). Evidence for the operation of another structural parameter has emerged from experiments where monoclonal, IgG antibodies (mAbs) specific for the α-subunit of the $Fc_\epsilon RI$ were used for cross-linking it directly on RBL-2H3 cells (Ortega et al., 1988). These mAbs bind with a stoichiometry of 1:1 Fab:$Fc_\epsilon RI$, hence causing the formation of only $Fc_\epsilon RI$ dimers. These mAbs designated F4, J17, and H10 were found to be effective secretagogues though differing in their efficiency. This provided the first unambiguous evidence that $Fc_\epsilon RI$ dimers can be sufficient for stimulating RBL-2H3 cells to secretion. A quantitative analysis of receptor dimerization as a function of these mAbs concentration clearly suggested that the cells' secretory response is determined not only by the number of $Fc_\epsilon RI$ dimers produced by each of the mAbs but even more so by their structural and dynamic properties. Some experiments carried out by our group (Ortega et al., 1988; Pecht et al., 1991a,b) suggested that orientational constraints imposed on the dimerized $Fc_\epsilon RI$ by the mAb may determine their secretion-inducing capacity.

In order to resolve the role of the relationship between the lifetimes of the $Fc_\epsilon RI$ dimers produced by these mAbs and the cellular response, we have recently measured the association and dissociation rates of Fab fragments derived from the above mAbs and of IgE to and from $Fc_\epsilon RI$ on the surface of live RBL-2H3 cells (Ortega et al., 1991). The minimal reaction scheme to which all these interaction kinetics could be fitted is one involving an initial formation of a $Fc_\epsilon RI$–ligand complex followed by its conformational transition from a low-affinity state l to a high-affinity state h. The equilibrium constant of this transition was found to be significantly larger than one for Fab-H10– and IgE–$Fc_\epsilon RI$ interactions at 25 °C. For Fab-F4 and Fab-J17 it is 0.05 and 0.2 at 25 °C, respectively, but increases at lower temperatures. This observation in particular suggested that it is the conformational transition of the $Fc_\epsilon RI$–ligand complexes which is responsible for the higher affinity and slow dissociation of IgE.

In order to directly address the question of relation between the lifetime of the $Fc_\epsilon RI$ dimers produced by the above mAbs and the cell's response we have now studied the interaction kinetics of the intact mAbs with the $Fc_\epsilon RI$ on live RBL-2H3 cells. The results provide a potential rationale for the dependence of the secretory response capacity to $Fc_\epsilon RI$–mAb dimers on three different parameters, namely, orientational constraints and lifetime of and conformational transitions in the dimers.

THEORETICAL BACKGROUND

Reaction Schemes. Analysis of the association and dissociation rates of the radioactively ^{125}I labeled mAbs to and from the $Fc_\epsilon RI$ on live cells takes advantage of earlier kinetic results of the corresponding Fab–$Fc_\epsilon RI$ interactions (Ortega et al., 1991). Thus the minimal model to which these data could be fitted involves two consecutive steps, namely, ligand binding to a low-affinity state l of the $Fc_\epsilon RI$ followed by a conformational transition into a higher affinity state h of the $Fc_\epsilon RI$–ligand complex. If one extends this model to the binding of intact, divalent mAbs to the $Fc_\epsilon RI$, the following reaction scheme emerges:

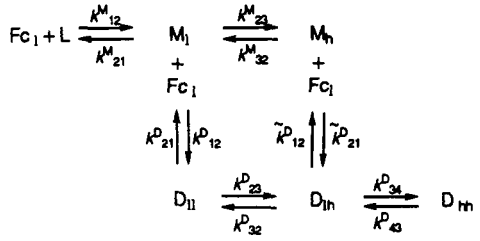

(1)

where L and Fc represent the ligand (i.e., the mAbs) employed and the free $Fc_\epsilon RI$ and M_l and M_h are the monomeric ligand–$Fc_\epsilon RI$ complexes in the low- and high-affinity states, respectively. The dimeric complex D_{ll} has both receptors in the l state, whereas D_{hh} exhibits two receptors in the h state. The hybrid D_{lh} has one receptor in the l state and the other in the h state. The k^l_{ij} terms (l = M, D; i, j = 1, 2, 3, 4) denote the rate constants of the respective reaction steps.

Some of the mAb dissociation experiments were performed by adding to the cells a large excess of unlabeled IgE in order to suppress reassociation of the labeled ligands. In that case the reaction scheme also involves

$$Fc_l + I \underset{k^I_{21}}{\overset{k^I_{12}}{\rightleftarrows}} M^I_l \underset{k^I_{32}}{\overset{k^I_{23}}{\rightleftarrows}} M^I_h \qquad (2)$$

where I represents the inhibitor, k^I_{12} and k^I_{21} represent its association and dissociation rate constants, and k^I_{23} and k^I_{32} represent the forward and reverse rate constants for the l → h transition of the IgE–$Fc_\epsilon RI$ complex.

In the following we confine ourselves to reactions 1 and 2. Thus we neglect changes of the $Fc_\epsilon RI$ and $Fc_\epsilon RI$–ligand concentrations by internalization and morphological changes of the cell's secretion because they are hardly observed at the temperatures where the kinetic experiments described in the present study were carried out (Oliver et al., 1988; Braunstein & Spudich, 1994; Kircheis et al., unpublished results).

Equilibrium Binding. Assuming that the different steps of reaction 1 are independent, the corresponding equilibrium concentration of bound mAbs can be calculated according to mass action law as follows:

$$[L]_b = 2K^M(K^M_c + 1)[Fc]_f[L]_f + 2K^D(1 + K^D_{c1} + K^D_{c1}K^D_{c2})K^M[L]_f[Fc]_f^2 \qquad (3)$$

where $K^M = k^M_{12}/k^M_{21}$, $K^M_c = k^M_{23}/k^M_{32}$, $K^D = k^D_{12}/k^D_{21}$, $K^D_{c1} = k^D_{23}/k^D_{32}$, and $K^D_{c2} = k^D_{34}/k^D_{43}$. $[L]_b$ and $[L]_f$ denote the molar concentrations of free and bound ligands, and $[Fc]_f$ is the molar concentration of free receptors.

$[Fc]_f$ and $[L]_f$ can be calculated from the corresponding total concentrations by utilizing the law of mass conservation:

$$[L]_T = [L]_f + 2K^M(K^M_c + 1)[L]_f[Fc]_f + 2K^D(1 + K^D_{c1} + K^D_{c1}K^D_{c2})K^M[L]_f[Fc]_f^2 \qquad (4a)$$

$$[Fc]_T = [Fc]_f + 2K^M(K^M_c + 1)[L]_f[Fc]_f + 4K^D(1 + K^D_{c1} + K^D_{c1}K^D_{c2})K^M[L]_f[Fc]_f^2 \qquad (4b)$$

where $[L]_T$ and $[Fc]_T$ are the total ligand and $Fc_\epsilon RI$ concentrations. The concentration of free $Fc_\epsilon RI$ in eqs 3 and 4 are normally expressed in terms of the average number of species/Å^2 of the cell surface. Consequently the equilibrium constant for dimer formation is formulated in units of Å^2. In

Chart 1[a]

$$\mathbf{A} = \begin{bmatrix} -2k^{M}_{12}{}^{+} & k^{M}_{21} & & & & & & & & \\ 2k^{M}_{12}{}^{+} & -(k^{M}_{21} + k^{M}_{23} + k^{D}_{12}{}^{+}) & k^{M}_{32} & k^{D}_{21} & & & & & & \\ & k^{M}_{23} & -(\tilde{k}^{D}_{12}{}^{+} + k^{M}_{32}) & & \tilde{k}^{D}_{21} & & & & & \\ & k^{D}_{12}{}^{+} & & -(k^{D}_{21} + k^{D}_{23}) & k^{D}_{32} & & & & & \\ & & & \tilde{k}^{D}_{12} + k^{D}_{23} & -(\tilde{k}^{D}_{21} + k^{D}_{32} + k^{D}_{34}) & & & & & \\ & & & & k^{D}_{34} & k^{D}_{43} & & & & \\ & & & & & & -k^{I}_{12}{}^{+} & k^{I}_{21} & & \\ & & & & & & k^{I}_{12}{}^{+} & -k^{I}_{21} - k^{I}_{23} & k^{I}_{32} & \\ & & & & & & & k^{I}_{23} & -k^{I}_{32} & \end{bmatrix}$$

[a] $k^{M}_{12}{}^{+} = [Fc]_f k^{M}_{12}$, $k^{D}_{12}{}^{+} = [Fc]_f k^{D}_{12}$, $\tilde{k}^{D}_{12}{}^{+} = [Fc]_f \tilde{k}^{D}_{12}$, and $k^{I}_{12}{}^{+} = [Fc]_f k^{I}_{12}$.

order to express all concentrations in the above equations in units of molarity, we make use of the expressions

$$[Fc]_f = [Fc]_f^* c_{cell} A/L \quad (5a)$$

$$k^D = k^{D*} L/(c_{cell} A) \quad (5b)$$

where $[Fc]_f^*$ is the surface density of Fc$_\epsilon$RI, k^{D*} is the corresponding association rate constant, c_{cell} and A denote the number of cells per unit volume and their average surface areas, respectively, and L is Avogadro's constant. k^D can be used to calculate the equilibrium constant K^D in eqs 3 and 4. Equation 5b shows that the rate constant k^D and hence the equilibrium constant K^D depend also on the cell concentration in the investigated sample. This must be taken into account when one compares k^D and K^D values from different experiments.

One should further consider that single cells may be heterogeneous in terms of their Fc$_\epsilon$RI density (Dower et al., 1981). In this case $[Fc]_f$ must be regarded as an average value while k^D and K^D are interpreted as effective parameters. The same holds if the cell surface is subdivided into different domains which do not freely exchange membrane components by diffusion (Sperotto & Mouritsen, 1991).

Kinetics of mAb Binding. The rate equations for reactions 1 and 2 can be written as

$$d\mathbf{L}/dt = \mathbf{A}\cdot\mathbf{L} \quad (6)$$

where

$$\mathbf{L} = ([L]_f, [M]_l, [M]_h, [D]_{ll}, [D]_{lh}, [D]_{hh}, [I]_f, [I]_l, [I]_h)$$

is a vector containing the concentrations of the free ligands $[L]_f$, the l- and h-state monomers ($[M]_l$ and $[M]_h$), the ll, lh, and hh dimers ($[D]_{ll}$, $[D]_{lh}$, and $[D]_{hh}$), the free inhibitor $[I]_f$, and the inhibitor–Fc$_\epsilon$I complex in the l and h states ($[I]_l$ and $[I]_h$). The corresponding matrix $\mathbf{A}$ is depicted in Chart 1.

Equation 6 is a set of nonlinear, coupled differential equations which can be solved by a seminumerical procedure outlined in the appendix. Thus, we obtain the concentrations of all species involved in reactions 1 and 2 as a function of time. The concentration of Fc$_\epsilon$RI-bound mAbs can then be calculated by

$$[L]_b(t) = [M]_l(t) + [M]_h(t) + [M]_l(t) + [D]_{ll}(t) + [D]_{lh}(t) + [D]_{hh}(t) \quad (7)$$

Our analysis of the mAb interaction kinetics is based on the assumption that the rate constants k^{M}_{12}, k^{I}_{12}, k^{M}_{21}, and k^{M}_{21} do not depend on the cell surface concentration of the free Fc$_\epsilon$RI. This has been justified by earlier experiments where association of IgE and Fab fragments of the mAbs, also employed in this study, were investigated (Ortega et al., 1991). Moreover, we assume that preaggregation of Fc$_\epsilon$RI on resting cells is negligibly small. This emerges from a recent study of the Fc$_\epsilon$RI distribution on RBL cells by fluorescence energy-transfer measurements (Kubitscheck et al., 1993).

MATERIALS AND METHODS

Cells. Rat mucosal mast cells of the secreting subline RBL-2H3 (Barsumian et al., 1981) were cultured in MEM containing 10% FCS, 2 mM glutamine, and antibiotics, at 37 °C, in a water-saturated atmosphere of 7% CO_2.

Monoclonal Antibodies. The preparation and characterization of Fc$_\epsilon$RI-specific mAbs F4, H10, and J17 have been described earlier (Ortega et al., 1988). Briefly, the hybridomas were obtained by fusing spleen cells from mice immunized intraperitoneally with RBL-2H3 cells, with NSO myeloma cells (ratio 5:1), essentially as described by Eshhar (1985). Selection was done by testing supernatants of the emerging hybridomas for their capacity to induce RBL-2H3 cell secretion. Positive clones were selected, retested, and cloned by limiting dilution. The selected clones were grown in tissue culture for production of mAbs. mAbs F4 (IgG_1), J17 (IgG_1), and H10 (IgG_{2b}) were purified from hybridoma culture supernatants by affinity chromatography on protein A–Sepharose columns (Pharmacia, Sweden). The mAbs were eluted from the column with 0.2 M glycine, pH 2.9. The eluate was collected directly into tubes containing neutralizing 2 M Tris buffer, pH 8.2, dialyzed against PBS, and stored frozen at −20 °C.

Mouse monoclonal IgE [A2 IgE, Rudolph et al. (1981)], specific for the 2,4-dinitrophenyl hapten, was purified from ascitic fluid by chromatography on DNP-BSA-Sepharose 4B columns.

Antibody concentrations were determined by their absorbance at 280 nm using $OD^{0.1\%}_{280\ nm} = 1.4$. For conversion to molar concentrations, MW 150 was assumed for the mAbs F4, H10, and J17 and MW 180 for IgE.

Measurements of Interaction Rates. In order to ascertain the cells' viability during the relatively long times of some experiments (up to 8 h), all rate measurements of binding or dissociation were carried out with the cells suspended in MEM containing 10% FCS and 20 mM HEPES, pH 7.4. Temperature was controlled by keeping the cell suspensions in thermostated water baths.

Association rates were measured by adding ^{125}I-labeled mAbs to cell suspensions [usually at (2–4) × 10^6 cells/mL],

preequilibrated at the specific temperature. The samples were thoroughly mixed, and at the indicated times, three aliquots of 150 μL were layered on 200 μL of FCS in microfuge tubes and immediately centrifuged for 20 s in a Beckman microfuge. The bottom of each tube containing the cell pellet was then cut and its radioactivity counted in a γ-counter.

For measuring the dissociation rates, cell suspensions [(10–20) × 10^6 cells/mL] were incubated with the labeled ligands for 1 h, during which the interactions reached equilibrium. Dissociation was then initiated by diluting the cell suspensions (usually 1:10, but sometimes less) with medium alone (DCD) or with medium containing the indicated concentrations of unlabeled IgE (DCDI). At the given times, three aliquots of 150 μL were transferred into microfuge tubes containing 200 μL of FCS and centrifuged immediately for 20 s. Again, the tubes were cut, and their bottoms containing the cell pellets were counted to determine the remaining cell-bound ligand. The concentration of bound ligand at the start of the experiment (time = 0) was determined on samples taken from the original cell suspension, immediately before dilution, and processed by the same protocol.

Dissociation of H10–Fc$_\epsilon$RI Complexes. In order to determine the concentration of the Fc$_\epsilon$RI which are no longer occupied by H10 after a 2-h dissociation period, we first incubated different cell suspensions [5 × 10^6 cells/mL] with a nearly saturating concentration of 4.8 × 10^{-9} M of intact unlabeled H10 (2 h). Dissociation was then induced by adding to these samples different concentrations of ^{125}I-labeled IgE. After an incubation time of 2 h the concentrations of bound [^{125}I]IgE were measured as described above.

The molar concentration of available Fc$_\epsilon$RI sites in each association and dissociation experiment was determined by incubating cell samples with a saturating concentration of ^{125}I-labeled IgE or Fab-H10 (usually 5 × 10^8 M) for at least 2 h and measuring the bound probe as before. Correction for nonspecific binding was done by subtracting the radioactivity associated with similar cell samples that were preincubated with >10^{-6} M unlabeled IgE for 1 h before addition of the labeled ligand.

In each experiment, the cell number in each sample used either for ligand binding kinetics or for the binding isotherms was directly determined by cell counting under the microscope. Variation among samples was minimal (less than 5%); hence no correction was deemed necessary. Also, no noticeable cell damage was evident upon microscopic examination. Still in some experiments cell viability was also checked by Trypan blue exclusion and found to be >90% at the end of the measurements.

β-Hexosaminidase Release. Where indicated, secretion from RBL-2H3 cells was monitored by following the activity of the granular enzyme β-hexosaminidase. To this end, cells were plated in 96-well plates (10^5 cells in 100 μL of MEM/well). On the following day, the monolayers were washed three times with Tyrode's buffer. After the treatment indicated for each experiment, secretion was allowed to proceed for the indicated time at 37 °C. From each well, two aliquots of 20 μL were transferred to a separate plate. To each of these samples was added 50 μL of substrate solution (1.3 mg/mL *p*-nitrophenyl-*N*-acetyl-β-D-glucosamine in 0.1 M citrate, pH 4.5), and the plates were incubated for 90 min at 37 °C. The reaction was stopped with 150 μL of stop solution (0.2 M glycine, pH 10.7). The color formed due to substrate hydrolysis was measured at 405 nm in an ELISA reader. To evaluate the total content of enzyme, cells in several control wells were lysed by 0.5% Triton X-100. The results are expressed as percent of the total β-hexosaminidase present in the cells. The release observed in the absence of sectretagogue (spontaneous release) was subtracted from each experimental value to yield the net percentage release.

Fitting Procedure. Equations 6 and A3 (appendix) were used to fit the rates of association and dissociation. To this end the rate constants $k^D{}_{12}$*, $k^D{}_{23}$, $k^D{}_{32}$, $k^D{}_{34}$, and $k^D{}_{43}$ were employed as free parameters. The rate constant $k^D{}_{21}$ of dimer dissociation was assumed to be twice the dissociation rate constant $k^M{}_{21}$ of the monomeric complex M_1. The dissociation rate constant $\tilde{k}^D{}_{21}$ was assumed to be identical with $k^D{}_{21}$ (cf. eq 1). The rate constants $k^M{}_{12}$, $k^M{}_{21}$, $k^M{}_{23}$, $k^M{}_{32}$, $k^I{}_{12}$, $k^I{}_{21}$, $k^I{}_{23}$, and $k^I{}_{32}$ were those derived earlier from the kinetics of Fab-F4, Fab-H10, Fab-J17 and IgE and were now used as fixed parameters. Because of the free energy conservation, the dimer formation rate constant $k^D{}_{12}$* is not an independent parameter in this case and can be calculated by

$$\tilde{k}^D{}_{12} = \frac{k^D{}_{12}k^D{}_{23}k^M{}_{32}\tilde{k}^D{}_{21}}{k^D{}_{21}k^D{}_{32}K^M{}_{23}} \tag{8}$$

The rate constants $k^I{}_{ij}$ (i, j = 1, 2, 3) for IgE–Fc$_\epsilon$RI interaction were taken from Ortega et al. (1991).

The computer fitting procedure employed the program MINUITL [CERN library, James and Ross (1975)], which contains several different minimizing subroutines enabling the search for a local minimum in the χ^2-function relating the experimental data and the computed values. In order to quantitate the quality of the fits, we calculated the error value f according to the equation

$$f = \{\sum_j ([L]_b(\mathrm{exp})_j - [L]_b(\mathrm{fit})_j)^2/(N\sigma_j)\}^{1/2} \tag{9}$$

where $[L]_b(\mathrm{exp})_j$ and $[L]_b(\mathrm{fit})_j$ denote the experimentally observed and the calculated concentrations of bound mAbs. N is the number of data points, and σ_j is the corresponding standard deviation of the respective experimental data from their mean value.

It should be mentioned that all fits to the dissociation rates were carried out in a self-consistent way in that the initial concentrations of bound mAbs were calculated by use of eqs 3 and 4 in which we inserted equilibrium constants K^M, $K^M{}_c$, K^D, $K^D{}_{c1}$ and $K^D{}_{c2}$ derived from the corresponding rate constants.

In order to estimate the statistical errors of the kinetic parameters, we calculated the normalized error value f/f_{min} as a function of the distinct rate constants $k^P{}_{ij}$ (P = M, D; i, j = 1, 2, 3, 4) in the vicinity of the respective minimum of the χ^2-function. The minimal f-value, $f^d{}_{min}$ at which the fit was found to be inappropriate, was used to calculate the statistical errors of the corresponding $k^P{}_{ij}$ by

$$\delta k^P{}_{ij} = \pm|k^P{}_{ij}(f_{min}) - k^P{}_{ij}(f^d{}_{min})| \tag{10}$$

RESULTS

The association and dissociation rates of mAbs F4, J17, and H10 to and from Fc$_\epsilon$RI on living RBL-2H3 cells were measured at three different temperatures, i.e., 25, 15, and 4 °C. The association experiments are labeled as ACs and the dissociation experiments as DCD (dissociation by dilution) and DCDI (dissociation by dilution and unlabeled IgE), respectively. For reasons of clarity we first present the results derived from the dissociation experiments and later proceed to the analysis of the corresponding ACs.

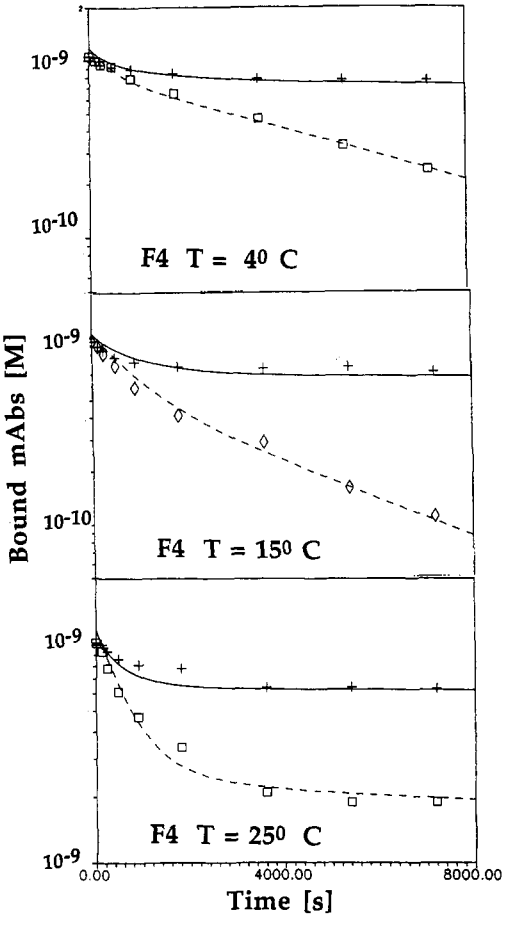

FIGURE 1: Time course of [^{125}I]F4 dissociation from FcεRI on RBL-2H3 cells in the presence (□, ◊: 1×10^{-7} M) and absence (+) of unlabeled IgE measured at 25 °C (upper panel), 15 °C (middle panel), and 4 °C (lower panel). Cells (7.5×10^6 cells/mL) were incubated with [^{125}I]F4 for 1 h at the respective temperatures. Dissociation was initiated by a 1:10 dilution of the cell suspension using medium with (□, ◊) and without (+) unlabeled IgE. At the indicated time the amount of bound [^{125}I]F4 was measured as described under Materials and Methods. The concentration of labeled F4 was adjusted to 2×10^{-8} M. The FcεRI concentration was 2.6×10^{-8} M before dilution. The lines result from fitting of the data to our kinetic model.

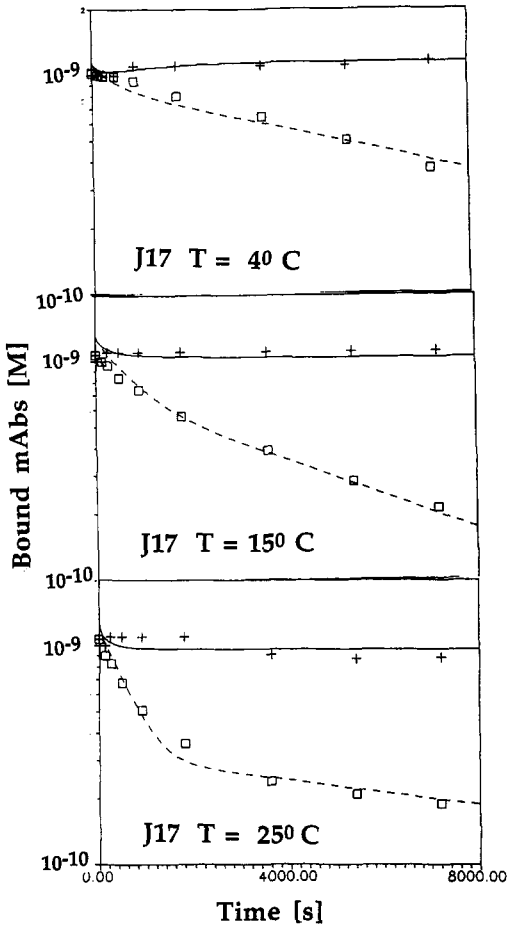

FIGURE 2: Time course of [^{125}I]J17 dissociation from FcεRI on RBL-2H3 cells in the presence (□: 1×10^{-7} M) and absence (+) of unlabeled IgE measured at 25 °C (upper panel), 15 °C (middle panel), and 4 °C (lower panel). Cells (7.5×10^6 cells/mL) were incubated with [^{125}I]J17 for 1 h at the respective temperatures. Dissociation was initiated by 1:10 dilution of the cell suspension using medium with (□) and without (+) unlabeled IgE. At the indicated time the amount of bound [^{125}I]J17 was measured as described under Materials and Methods. The concentration of labeled J17 was adjusted to 2×10^{-8} M. The FcεRI concentration was 2.66×10^{-8} M before dilution. The lines result from fitting of the data to our kinetic model.

Kinetics of mAb–FcεRI Interaction. Figures 1 and 2 display semilogarithmic plots of the DCDs and DCDIs of J17 and F4 measured at the indicated temperatures. They show that the dissociation time course cannot be fitted to a monoexponential function. This suggests that more than a single step is involved in that dissociation process, one of which is rather slow and does not reach completion even after 160 min.

In the first data-fitting cycle we assumed that the forward and reverse rate constants for the l → h transition of one mAbs–receptor pair are identical in the monomeric and dimeric complex. Hence we impose the following restrictions on our fitting parameters:

$$k^{D}_{23} = 2k^{M}_{23} \tag{11a}$$

$$k^{D}_{32} = k^{M}_{32} \tag{11b}$$

$$k^{D}_{34} = k^{M}_{23} \tag{11c}$$

$$k^{D}_{43} = 2k^{M}_{32} \tag{11d}$$

The corresponding equilibrium constants would then read as

$$K^{D}_{c1} = 2K^{M}_{c} \tag{12a}$$

$$K^{D}_{c2} = K^{D}_{c1}/2 \tag{12b}$$

This enabled us to fit the initial, fast phase of all DCDs and DCDIs of F4 and J17. In addition we could reproduce the respective slow phases observed at 4 °C. At 25 °C, however, all fitting trials predicted a much faster dissociation than indicated by our data, while at 15 °C only moderate deviations from the experimental data were observed. Therefore, in a second cycle of analysis, we relaxed conditions 10c and 10d, thus allowing k^{D}_{34} and k^{D}_{43} to be free parameters in the fit. This led to a satisfactory fitting of all corresponding DCDs and DCDIs in terms of the very same parameters (solid and dashed curves in Figure 1, respectively). Fine-tuning of the fits was sometimes achieved by allowing small deviations from the k^{D}_{23} and k^{D}_{32} dictated by eqs 11a and 11b and from the k^{M}_{12} values reported by Ortega et al. (1991). The thus obtained rate constants are listed in Table 1.[2]

The rate constant k^{D}_{43} was found to be significantly lower than its expected value at 25 and 15 °C. This particularly

[2] Since association and dissociation experiments were performed with different cell concentrations, only the dimerization rate constants k^{D}_{12}* in Table 1 can be used for comparing the corresponding fits (cf. eq 5b in the theory section).

Table 1

A. Rate Constants Derived from the Fits to the DCDs, DCDIs, and ACs of F4, J17, and H10[a]

parameter	T (°C)	expt[b]	F4	J17	H10	parameter	T (°C)	expt[b]	F4	J17	H10
k^{M}_{12} [(M^{-1} s^{-1}) × 10^5]	25	D	1.6	6.0	5.0	k^{D}_{12}* [($Å^{-2}$ s^{-1}) × 10^3]	25	D	4.6	51.0	230.0
	25	A	1.8	6.0	5.0		25	A	3.1	70.0	470.0
	15	D	1.1	6.0			15	D	4.6	51.0	
	15	A	1.5	6.0			15	A	5.5	39.0	
	4	D	0.65	5.0			4	D	4.6	51.0	
	4	A	0.80	5.0			4	A	5.5	54.0	
k^{M}_{12} (s^{-1} × 10^{-3})	25	D	10.0	25.0	5.0	k^{D}_{23} (s^{-1} × 10^{-3})	25	A	0.4	0.25	0.6
	25	A	5.0	18.0	5.0		25	A	0.4	0.12	0.6
	15	D	5.0	20.0			15	D	1.0	1.0	
	15	A	7.0	20.0			15	A	1.0	1.0	
	4	D	5.0	10.0			4	D	1.9	2.0	
	4	A	8.0	10.0			4	A	1.9	2.0	
k^{M}_{23} (s^{-1} × 10^{-4})	25	D	2.5	0.9	1.6 × 10^4	k^{D}_{32} (s^{-1} × 10^{-3})	25	D	1.0	1.8	1.7
	25	A	2.5	0.9	1.6 × 10^4		25	A	1.0	1.0	1.7
	15	D	5.0	6.0			15	D	0.5	1.5	
	15	A	5.0	6.0			15	A	0.5	1.5	
	4	D	8.0	10.0			4	D	0.4	0.8	
	4	A	8.0	10.0			4	A	0.4	0.8	
k^{M}_{32} (s^{-1} × 10^{-4})	25	D	10.0	18.0	50.0	k^{D}_{34} (s^{-1} × 10^{-4})	25	D	0.19	1.6	
	25	A	10.0	18.0	50.0		25	A	0.19	0.5	
	15	D	5.0	15.0			15	D	4.0	4.0	
	15	A	5.0	15.0			15	A	4.0	4.0	
	4	D	4.0	8.0			4	D	15.0	20.0	
	4	A	4.0	8.0			4	A	18.0	10.0	
k^{D}_{12} [(M^{-1} s^{-1}) × 10^8]	25	D	0.18	2.0	90.0	k^{D}_{43} (s^{-1} × 10^{-4})	25	D	0.23	0.7	
	25	A	0.04	0.9	6.0		25	A	0.23	0.7	
	15	D	0.18	2.0			15	D	4.0	2.2	
	15	A	0.07	1.6			15	A	5.0	2.2	
	4	D	0.18	2.0			4	D	6.4	7.0	
	4	A	0.07	1.6			4	A	6.4	7.0	

B. Equilibrium Constants of the mAb–Fc_ϵRI Interactions Derived from the Rate Constants in Table 1A and from Earlier Analyses of Binding Isotherms at 25 °C (Ortega et al., 1988)

parameter	T (°C)	expt[b]	F4	J17	H10	parameter	T (°C)	expt[b]	F4	J17	H10
K^{M} (M^{-1} × 10^7)	25	D	1.6	2.4	10	K^{D*} ($Å^2$ × 10^6)	25	D	0.23	1.1	76
	25	A	3.6	3.7	20		25	A	0.16	2.2	1.5 × 10^2
	25	O	1.0	1.8	20		25	O	0.05	1.5	1.5 × 10^3
	15	D	2.2	3.0			15	D	0.45	1.3	
	15	A	2.1	3.1			15	A	0.39	1.0	
	4	D	1.3	5.0			4	D	0.46	2.6	
	4	A	1.0	5.0			4	A	0.85	1.8	
K^{M}_{c}	25	D	0.25	0.05	3 × 10^2	K^{D}_{c1}	25	D	0.4	0.14	0.35
	25	A	0.25	0.05	3 × 10^2		25	A	0.4	0.12	0.35
	25	O	0.25	0.05	3 × 10^2		25	O	0.4	0.12	0.35
	15	D	1.0	0.4			15	D	2.0	0.66	
	15	A	1.0	0.4			15	A	2.0	0.66	
	4	D	2.0	1.25			4	D	4.7	2.5	
	4	A	2.0	1.25			4	A	4.7	2.5	
K^{D} (M^{-1} × 10^9)	25	D	0.9	4.0	3 × 10^2	K^{D}_{c2}	25	D	0.82	2.28	
	25	A	0.2	2.8	2 × 10^2		25	A	0.82	1.20	
	25	O	0.04	1.3	1 × 10^4		25	O	0.82	1.20	
	15	D	1.8	5.0			15	D	1.0	1.80	
	15	A	0.5	1.2			15	A	0.8	1.8	
	4	D	1.8	10.0			4	D	2.3	2.8	
	4	A	1.1	2.6			4	A	2.8	1.4	

C. Rate Constants of the Interaction between Fc_ϵRI and the mAbs F4 and J17 Estimated from the Extrapolation of the Corresponding Arrhenius Plots in Figure 7

parameter	F4	J17	parameter	F4	J17
k^{M}_{12} [(M^{-1} s^{-1}) × 10^5]	1.6	6.0	k^{D}_{23} (s^{-1} × 10^{-4})	2.2	0.72
k^{M}_{21} (s^{-1} × 10^{-2})	1.2	2.5	k^{D}_{32} (s^{-1} × 10^{-3})	1.1	3.0
k^{M}_{23} (s^{-1} × 10^{-4})	2.0	0.55	k^{D}_{34} (s^{-1} × 10^{-4})	0.61	0.23
k^{M}_{32} (s^{-1} × 10^{-3})	1.5	1.5	k^{D}_{43} (s^{-1} × 10^{-4})	0.53	0.45
k^{D}_{12} [(M^{-1} s^{-1}) × 10^8]	0.18	2.0			

[a] The standard deviation of the values for the rate constants is in the range between 10% and 40%. [b] A: measurement of association rates. D: measurement of dissociation rates. O: data from Ortega et al. (1988).

holds for T = 25 °C where k^{D}_{43} is 2.3 × 10^{-5} s^{-1} for Fc_ϵ–F4–Fc_ϵ and 7 × 10^{-5} s^{-1} for Fc_ϵ–J17–Fc_ϵ (the corresponding k^{M}_{32} values are 1 × 10^{-3} and 1.2 × 10^{-3}, respectively). Thus, the corresponding equilibrium constant K^{D}_{c2} becomes considerably larger than that of the preceding $D_{ll} \leftrightarrow D_{lh}$ transition (i.e., K^{D}_{c1}), in contrast to the prediction of eq 12. As a consequence, a larger fraction of Fc_ϵRI dimers dissociate quite slowly, as indicated by the DCDIs in Figure 1.

The DCD and DCDI results obtained for H10 are less informative than the corresponding data sets of F4 and J17.

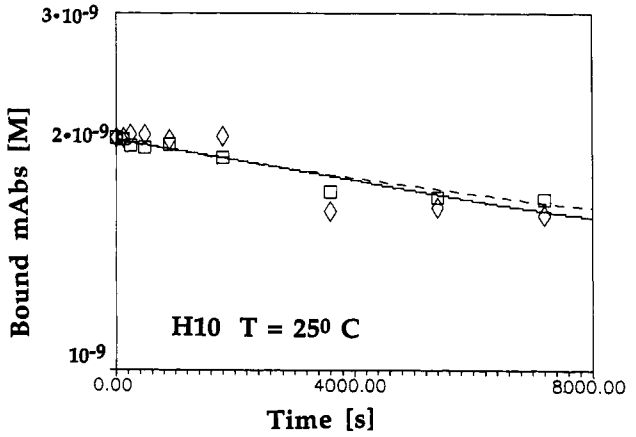

FIGURE 3: Time course of [^{125}I]H10 dissociation from FcεRI on RBL-2H3 cells in the presence (□: 1×10^{-7} M) and absence (◊) of unlabeled IgE measured at 25 °C. Cells (7.5×10^6 cells/mL) were incubated with [^{125}I]H10 for 1 h at the respective temperatures. Dissociation was initiated by 1:10 dilution of the cell suspension using medium with (□) and without (◊) unlabeled IgE. At the indicated time the amount of bound [^{125}I]H10 was measured as described under Materials and Methods. The concentration of labeled H10 was adjusted to 2.54×10^{-8} M. The FcεRI concentration was 2.66×10^{-8} M before dilution. The solid and dashed lines result from fitting of DCD and DCDI to our kinetic model.

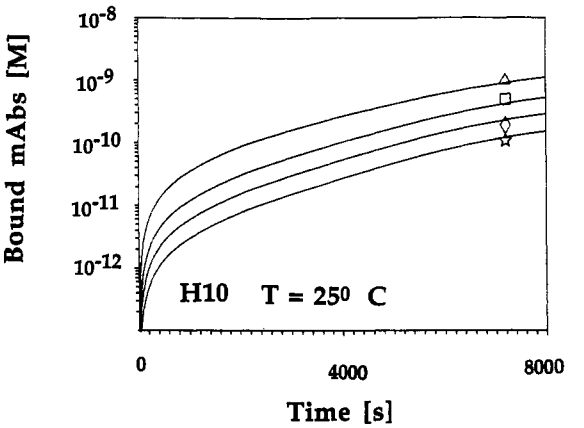

FIGURE 4: Calculated time course of IgE association to cell resident FcεRI at 25 °C after a 2-h incubation with unlabeled, intact H10 (2.54×10^8 M). The calculation was done using the kinetic parameters derived from dissociation experiments with H10 and IgE and was repeated for four different IgE concentrations (i.e., 5×10^{-9}, 1×10^{-8}, 2×10^{-8}, and 5×10^{-8} M). Comparison with experiment was achieved by measuring the concentration of bound [^{125}I]IgE after another 2 h of incubation with the above total [^{125}I]IgE concentrations (indicated by ☆, ◊, □, and △, respectively).

In analogy to what has been observed for its Fab fragments (Ortega et al., 1991), mAb H10 dissociates rather slowly from the FcεRI (Figure 3).[3] While the addition of IgE usually caused a significant acceleration of mAb dissociation (as observed for F4 and J17, Figures 1 and 2), the DCDI values of H10 become slightly larger than the corresponding DCD values after 4×10^3 s. This surprising observation was reproduced in two independent further dissociation experiments carried out on different cell batches.

An analysis of H10 dissociation (Figure 3) in terms of our two-state model reveals that the above effect can be accounted for by assuming that the l → h transition in the dimeric complex proceeds at least orders of magnitude slower than the corresponding reaction of the monomer ($k^{D}_{23} \ll k^{M}_{23}$). In this case the dimer dissociation is determined by k^{D}_{21}. It therefore proceeds comparatively fast, but subsequently, the monomeric Fc–H10 complex switches predominantly into the high-affinity h state, from which the ligand does not dissociate in the fast time domain. Thus the concentration of bound ligands is only slightly reduced in the time regime of our experiment. If one initiates dissociation solely by dilution, some re-formation of receptor dimers may occur, whereas this is inhibited in the DCDI experiments. Since dimer formation reduces the ratio of bound ligands to occupied FcεRI, the dissociation caused by dilution may be slightly faster than that observed in the corresponding DCDI experiments.

The solid (DCD) and dashed (DCDI) lines in Figure 3 result from the fit of this model to the experimental data. The respective parameter values are given in Table 1A. Due to the scattering in the experimental data, the fit is not as good, but accounts, at least qualitatively, for the observed behavior of both dissociation processes.

In order to examine the validity of our interpretation of the H10 dissociation, we performed the following experiment: First we incubated different cell samples with a saturating amount of unlabeled, intact H10. After an incubation time of 90 min we added different concentrations of [^{125}I]IgE. The concentration of [^{125}I]IgE bound to FcεRI was then determined after an incubation time of 2 h. The thus obtained data are shown in Figure 4. We now utilized the fit parameters derived from the DCDI of H10 to calculate the time course of IgE binding to cells which have been saturated with unlabeled H10 for the different IgE concentrations employed in the above experiments. As shown in Figure 4 this procedure reproduced the experimental data in a satisfactory way.

We have also performed a similar experiment in which we incubated different cell samples with unlabeled Fab fragments of H10. In this case only 10% of the FcεRI were found to be ligated by [^{125}I]IgE after 2 h (data not shown). This finding corroborates the notion that a major part of the Fab-H10–FcεRI complexes exist in the high-affinity h state, from which they do not dissociate in that time domain (Ortega et al., 1991), and supports our interpretation of the mAb-H10 dissociation kinetics.

While the DCDs and DCDIs provide detailed information even for different steps involved in the dissociation process, the ACs are less informative. This is because the apparent association rates are determined by the slowest step involved in the reaction scheme. All steps proceeding faster cannot be derived in an unambiguous way from the data. The ACs can be used, however, to check whether the rate constants derived from the fits to the corresponding dissociation rates also describe well the association process.

To this end we first fitted the ACs using all rate constants derived from the fits to the DCDs and DCDIs as fixed parameters. This yielded satisfactory approximations to the experimental data. The final fits displayed by solid lines in Figure 5 are obtained by allowing some variations of the parameters (cf. Table 1A). This demonstrates that our model describes the association and dissociation of the three mAbs in an internally consistent way.

The rate constants presented in Table 1A were used to calculate the equilibrium constants of the different reaction steps, which are listed in Table 1B. For comparison this table also presents the respective equilibrium constants derived from the data of Ortega et al. (1988) for F4, J17, and H10 at 25 °C.[4] In this study we did not consider possible conformational transitions of the receptor–ligand complex. The original binding constants K_r and K_d must therefore be regarded as

[3] Since H10 dissociation does not show a significant temperature dependence, only the data observed at 25 °C are shown.

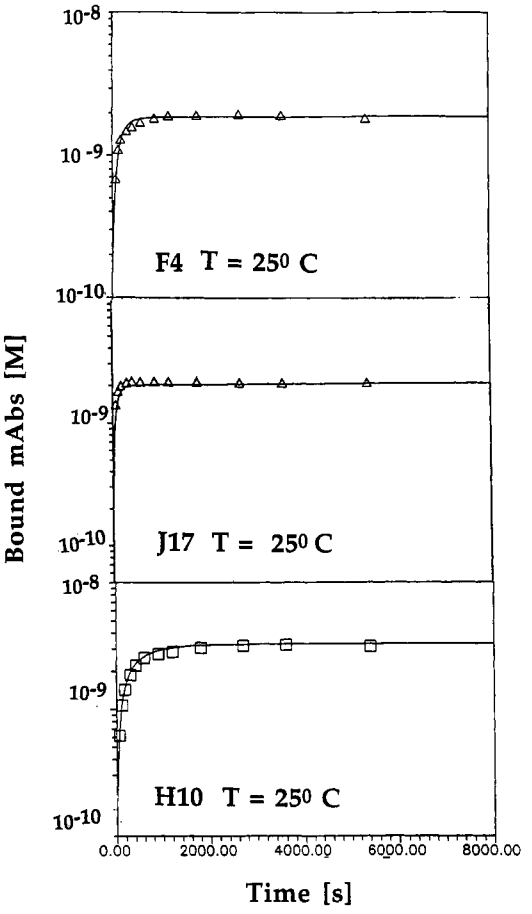

FIGURE 5: Time course of [^{125}I]F4, [^{125}I]J17, and [^{125}I]H10 association to cell resident Fc$_\epsilon$RI measured at 25 °C. The radioactively labeled ligands were added to cell suspensions (4.2×10^6 cells/mL). After the indicated time, the concentration of bound proteins was measured as described under Materials and Methods. The ligand concentrations were adjusted to 2.7×10^{-9} M (F4), 8.6×10^{-9} M (J17), and 3.8×10^{-9} M (H10). The Fc$_\epsilon$RI concentration was 8.57×10^{-9} M for all experiments.

Table 2: Parameters Derived from the Fits to the Release Kinetics in Figure 6

parameter	F4	J17	H10
σ_0 ($s^{-1} \times 10^{-3}$)	6.0 ± 0.5	9.0 ± 1	2.2 ± 0.5
f_R	0.81	0.81	0.81
Γ ($M^{-1} \times 10^{12}$)	4.0 ± 0.5	4.0 ± 0.5	4.0 ± 0.5
n	2.0 ± 0.3	2.0 ± 0.3	2.0 ± 0.3
θ_0 ($s^{-1} \times 10^{-3}$)	2.5 ± 0.3	1.2 ± 0.2	2.5 ± 0.3
τ ($M^{-1} \times 10^{11}$)	2.8 ± 0.2	0.7 ± 0.05	7.5 ± 0.5
m	1.2 ± 0.05	1.2 ± 0.05	1.2 ± 0.05

effective parameters, which relate to K^M and K^D by the expressions $K^M = K_r^a/(1 + K_c)$ and $K^D = K_d/(1 + K_{c1} + K_{c1}K_{c2})$, provided that $K_c \ll 1$. If the latter condition is not fulfilled, the fit to the one-step model yields unreasonable values for the binding constants.

Consequently, for F4 and J17 the K^M and K^D values emerging from the analysis of Ortega et al. (1988) are close to the corresponding parameters obtained in the present study, whereas we found significant deviations for the parameter values of H10 (cf. Table 2).

Kinetics of Mediator Release. Finally we have measured the time course of β-hexosaminidase secretion as a monitor for the cells' secretory response to each of the three mAbs employed. These experiments were done at four different ligand concentrations. The results are displayed in Figure 6 (only two data sets are shown for H10). Clearly the significant differences among the corresponding secretory response patterns observed in earlier studies were reproduced (Ortega et al., 1988; Pecht et al., 1989). The kinetics and the maximal levels of secretion induced by J17 and F4 exhibit a marked dependence on ligand concentration. This dependence is apparently less pronounced for H10. This observation and the relationship between dimer formation and the time course of secretion are discussed below.

[4] It should be noted that the K_d values in Table 1 of Ortega et al. (1988) are expressed in units of 10^4 M rather than in M, as indicated in the respective legend.

Table 3: Activation Enthalpies as Derived from the Arrhenius Plots of the Rate Constants k^D_{ij}

	F4	J17
H^D_{23} (kJ/mol)	−44.0	−73.9
H^D_{32} (kJ/mol)	22.4	28.0
H^D_{34} (kJ/mol)	−125.5	−83.9
H^D_{43} (kJ/mol)	−72.3	−60.9

DISCUSSION

Correlation between Kinetics of Fc$_\epsilon$RI Dimerization and the Cell's Secretory Response. We investigated the kinetics of the Fc$_\epsilon$R dimerization process by specific mAbs in order to resolve the parameters which determine the cellular response to these Fc$_\epsilon$R clusters. DeLisi (1981) has formulated a theoretical relation between the lifetime of such clusters and their secretion-stimulating capacity. It assumed that Fc$_\epsilon$RI must remain in close proximity for a minimal length of time in order to provide stimulation. This may, for example, reflect the time required for attaining a sufficient steady-state level of a coupling element (e.g., a second messenger concentration or an activated protein kinase). Thus we looked for a possible correlation between the lifetime of the Fc$_\epsilon$RI dimers produced by the employed mAbs and their capacity to initiate the cell's secretory response. This was done as follows: First, we evaluated the kinetic parameters of reaction 1 at physiological temperature by extrapolating the corresponding Arrhenius plots of J17 and F4 to 37 °C (cf. Figure 7); a more detailed discussion of these plots is given in the next paragraph of this section). These parameters are listed in Table 1C. Since both association and dissociation rates of H10 to and from the Fc$_\epsilon$RI were found to exhibit a rather low temperature dependence, the corresponding parameters obtained at 25 °C were used for this mAb. Second, these parameters were employed for calculating the time course of forming the different dimer states D_{ll}, D_{lh}, and D_{hh} using the same receptor and mAb concentrations employed in the release experiments. Third, we utilized a mathematical model designed by Dembo et al. (1979) to calculate the secretory response as a function of time and ligand concentrations.

Dembo et al. (1979) proposed that histamine or other releasable mediators appear in discrete "quanta" so that the secretory response can be described as a stochastic process. The secretion time course can therefore be derived from the following differential equation:

$$dQ_R(t)/dt = -F(Q_R(t))\, P_R([D^*]) \qquad (13a)$$

where

$$F(Q_R) = Q_R(t)(1 + \beta Q_R(t))/(1 + 1/2\beta) \qquad (13b)$$

$$Q_R(0) = 1 \qquad (13c)$$

and $Q_R(t)$ is the fraction of the releasable β-hexosaminidase remaining in the cells at time t. P_R is the rate constant of the secretory process, and it depends on the concentration of active Fc$_\epsilon$RI dimers [D*]. β is an empirical parameter, which accounts in the theory of Dembo et al. (1979) for the possibility that the above quanta may interact with each other in order to enhance ($\beta > 0$) or inhibit release ($\beta < 0$). In our calculation we neglected this interaction. The experimentally measured quantity is the released fraction $H_R(t)$ of the cell's total β-hexosaminidase activity content f_R at time t. It is given by

$$H_R(t) = f_R(1 - Q_R(t)) \quad (14)$$

The exact analytical expression for the function $P_R([D^*])$ is not available. Some features of the degranulation process can, however, be used to construct a suitable empirical model function, i.e.: (i) $P_R = 0$ in the absence of clustered Fc$_\epsilon$RI; (ii) P_R increases monotonously with the concentration of stimulating Fc$_\epsilon$RI clusters; (iii) P_R increases weakly at low concentrations of stimulating clusters; and (iv) it saturates at high concentrations of Fc$_\epsilon$RI clusters. All of these observations are accounted for if P_R is parametrized by the following Hill function:

$$P_R([D^*]) = \sigma_0([D]/\Gamma)^n/(1 + ([D^*]/\Gamma)^n) \quad (15)$$

where σ_0 denotes the rate of the release process when the cell contains one-half of its initial releasable content, Γ is the Fc$_\epsilon$RI dimer concentration for which the release probability is half-maximal, and n is the empirical Hill coefficient. Equation 13a is a part of a system of coupled differential equations (in addition to eq 6). In a numerical procedure we subdivided the time course of the secretory processes into time intervals dt_j (cf. appendix). In each interval, the corresponding concentration of stimulating dimers $[D^*]_j$ is approximately time independent. Hence Q_{Rj} can be derived by a simple integration of eq 13a. This yields:

$$Q_{Rj} = Q_{Rj-1} \exp\{-P_R([D^*])_j\, dt_j\} \quad (16)$$

The theory described so far only accounts for the stimulation of the cells by clustered Fc$_\epsilon$RI. It is known, however, that desensitization of the cells is also taking place, e.g., at a high level of Fc$_\epsilon$RI cross-linking (Kagey-Sobotka et al., 1981; Dembo et al., 1979; Goldstein et al., 1979; DeLisi and Siraganian, 1979; Pecht et al., 1991a). It was shown earlier by Ortega et al. (1988) that the dose–response curves of RBL-2H3 cells to mAbs F4, J17, and H10 are asymmetric and do not correlate simply with the dimer concentrations. Already this indicates that desensitization is also operative in RBL-2H3 cells. It becomes more apparent when the cells are equilibrated with mAb F4 under conditions which are nonpermissive for degranulation, i.e., at low temperatures (25 °C) or in the absence of extracellular calcium. The maximal observed release after exposure to permissive conditions is much lower than that induced by stimulating the cells under permissive conditions (Pecht et al., 1991a). Dembo et al. (1979) have modeled desensitization of human basophils in terms of an enzymatic reaction stimulated by clustered Fc$_\epsilon$RI. We are using a less concrete model in that we solely assume that the probability coefficient σ_0 in eq 15 is a parameter which decreases upon desensitization according to

$$\sigma_{0j} = \sigma_{0j-1} \exp(-\theta([D])\, dt_j) \quad (17)$$

where the apparent decay constant $\theta([D])$ is given by the Hill function,

$$\theta([D]) = \theta_0(\tau[D])^m/(1 + (\tau[D])^m) \quad (18)$$

where θ_0 denotes the desensitization probability per unit time and τ is the dimer concentration at which the desensitization probability is half maximal. [D] is the total dimer concentration, which is assumed to be constant in the time interval dt_j. m is the Hill coefficient. Equation 18 describes desensitization as being limited at low [D] and reaching a plateau value at higher [D] values. This is in accordance with the dose–response curves in particular to mAb J17 and F4, which exhibit their maxima at ligand concentrations lower than the corresponding values required for maximal dimer formation (Ortega et al., 1988).

In a first attempt to fit the secretion data (Figure 6) we assumed that already the D_{ll} conformer of the Fc$_\epsilon$RI dimers causes secretion. Hence σ_0, θ_0, Γ, τ, f_R, m, and n were used as free parameters. While several data sets obtained with mAb F4 (Figure 6b) could be reproduced very well, significant discrepancies were obtained for J17 and H10. Therefore in a second round of fitting we only considered the dimeric species D_{lh} and D_{hh}. This procedure yielded rather satisfactory fits to all the data sets obtained for F4 and H10 as illustrated by the solid lines in Figure 6b,c. Some systematic deviations are noted from the initial phase of the release time course induced by high J17 concentrations (panels A and B of Figure 6a), but these discrepancies should be considered as minor in view of the simplicity of the model employed. The results of the above fitting procedures suggest that only Fc$_\epsilon$RI dimers having at least one receptor in the high-affinity h state can initiate secretion. As a consequence, the time course of the latter process is predominantly determined by the rate of D_{lh} formation, which is given by $k^D_{23} + k^D_{32}$. It is remarkable that all secretion time-course curves obtained for a given mAb could then be fitted using the very same set of parameter values (Table 2). Even small changes in these parameters yielded significant deviations from the experimental data. The same Hill coefficients and identical f_R values were used for fitting all secretion time-course curves. The stimulatory probability σ_0 is practically identical for J17 and F4 (i.e., 8×10^{-3} and 6×10^{-3} s^{-1}, respectively), whereas the corresponding parameter value for H10 is slightly lower (2×10^{-3} s^{-1}). Interestingly, these results suggest that the three mAbs differ mainly in the parameters determining the respective desensitization. The stimulation rate constant, which is the net result of the rates of the coupling processes, is affected by the desensitization process approximated by the parameter θ_0, which is identical for H10 and F4 (2.5×10^{-3} s^{-1}), but much higher for J17 (1.2×10^{-2} s^{-1}). The coupling between dimer formation and desensization (τ) decreases in the order H10 > F4 > J17.

Taken together the above results provide evidence that corresponding dimer conformers (i.e., D_{ll}, D_{lh}, and D_{hh}) formed by the mAbs employed differ in structural and functional terms. This is first of all reflected by their different rate constants k^d_{23}, k^d_{32}, k^d_{34}, and k^d_{43} (cf. Table 1). The Fc$_\epsilon$RI dimers produced by each of the different mAbs are expected to have their distinct individual structures dictated by the epitope and the way they are bound by the respective mAb. We have earlier tried to rationalize the distinct secretory dose–response patterns to the mAbs in terms of these orientational constraints. Now the (probability) coefficient σ_0 (eq 15), which was assumed to decrease upon desensitization (eq 17), reflects the coupling efficiency that distinct Fc$_\epsilon$RI dimers are endowed with.

In this context it is noteworthy that the above model for the coupling between Fc$_\epsilon$RI dimerization and secretory response

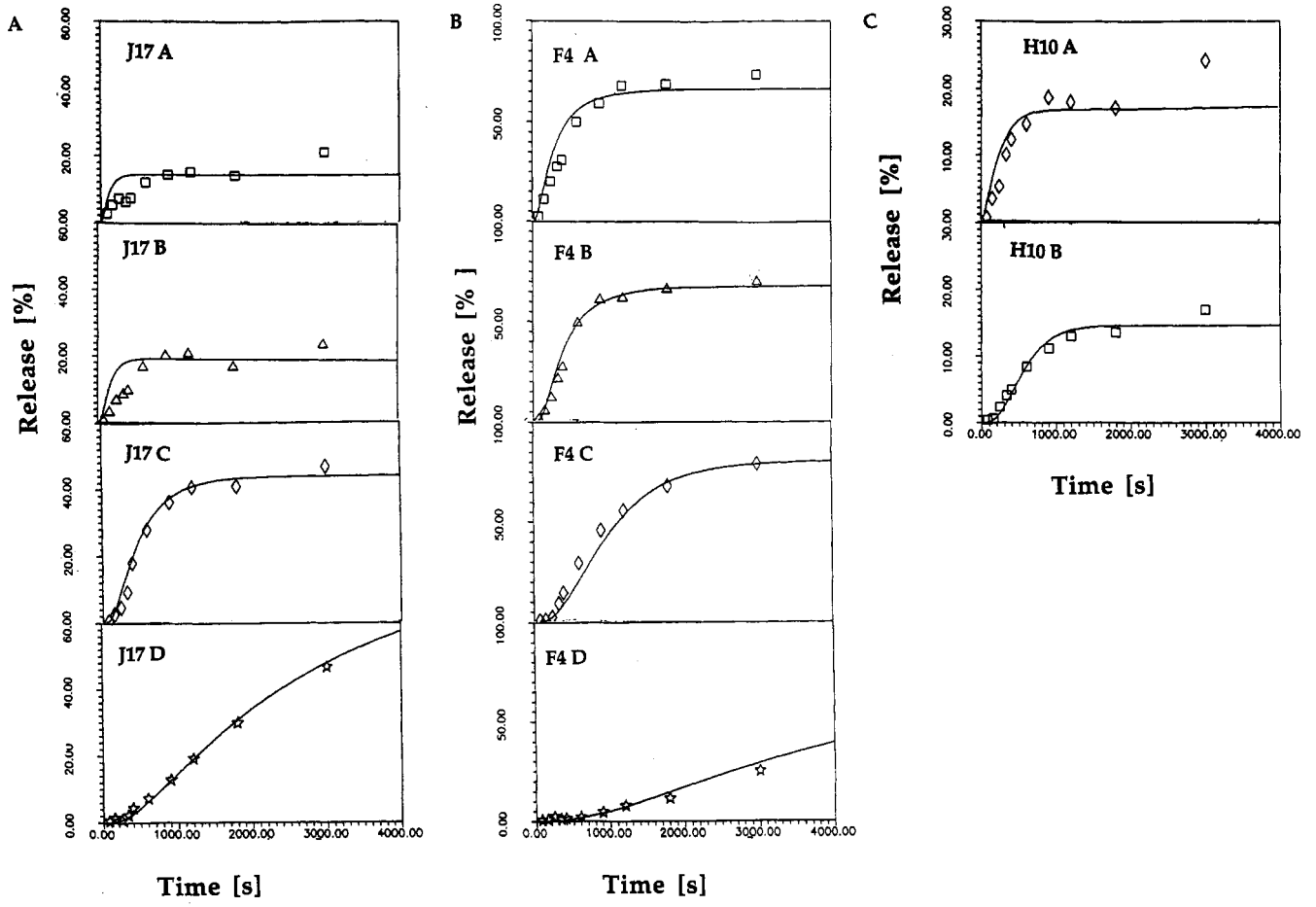

FIGURE 6: Time course of mediator secretion by RBL-2H3 cells induced upon cross-linking their $Fc_\epsilon RI$ by (a) F4, (b) J17, and (c) H10. The concentrations of cross-linking mAbs were (A) 10^{-7} M, (B) 10^{-8} M, (C) 10^{-9} M, and (D) 10^{-10} M for J17 and F4 and (A) 2×10^{-8} M and (B) 2×10^{-10} M for H10. The $Fc_\epsilon RI$ concentration was determined by IgE binding to 3×10^{-10} M. The β-hexosaminidase secretion was measured as described under Materials and Methods. The solid lines result from the fitting procedure described in the discussion.

is also supported by another type of experiment (Pecht et al., 1991a): RBL-2H3 cells were first incubated with suboptimal concentrations of J17 and H10 for 30 min at 37 °C. The cells were washed and then further incubated with polyclonal antibodies specific for mouse IgG for another 30 min at the same temperature. No further secretion could be observed as the result of the more extensive clustering the $Fc_\epsilon RI$ dimers. This is most probably caused by desensitization of the cells in accordance with the expectations from the present analysis.

It should be emphasized that at present the biochemical processes underlying the above phenomena are still largely unknown. Resolution of the intricate cascade of, e.g., transient phosphorylation–dephosphorylation of specific cell components is only in its emergence and would hopefully provide the required understanding of molecular details. At present the determined parameters should therefore be solely regarded as means to characterize the different capacities of the mAbs employed to cause secretion and desensitization of the cells.

The following conclusions can be drawn from the findings: (i) The secretory response of RBL-2H3 cells to mAbs F4, J17, and H10 requires formation of dimers where at least one $Fc_\epsilon RI$ is in the h state (D_{lh} species). In order to examine whether and how the dimers' lifetime is relevant to their stimulatory capacity, we compared the lifetimes of the different $Fc_\epsilon RI$ dimeric species at 37 °C. Due to the relatively fast diffusion of the $Fc_\epsilon RI$ on mast cells (DeLisi, 1981), the lifetime τ_D of D_{ll} is given as $1/k^D_{21}$. Using the respective parameters for F4 and J17 and H10 (Table 1) ($k^D_{12} = 2k^M_{12}$), one obtains τ_D = 41, 33, and 100 s for these mAbs, respectively. The lifetimes of dimers in the lh and hh states can be estimated by use of the equations (DeLisi, 1980)

$$\tau_D(D_{lh}) = (k^D_{23} + k^D_{21})/k^D_{21}k^D_{32} \quad (19a)$$

$$\tau_D(D_{hh}) = (k^D_{23} + k^D_{21})(k^D_{34} + k^D_{32})/k^D_{21}k^D_{32}k^D_{43} \quad (19b)$$

Thus, one obtains $\tau_D(D_{lh})$ = 910 s (F4), 333 s (J17), and 588 s (H10) and $\tau_D(D_{hh}) = 1.8 \times 10^4$ s (F4) and 2.2×10^4 s (J17). This shows that the l → h transition within the dimers, which is required for the initiation of the secretory response, significantly prolongs the lifetime of these active species. Hence our results support the notion (DeLisi, 1981) that $Fc_\epsilon RI$ clusters must have a comparatively long (i.e., $>10^2$ s) lifetime in order to provide triggering of the secretory response. $Fc_\epsilon RI$ clusters formed by cross-linking $Fc_\epsilon RI$-bound IgE by divalent haptens exhibit a much shorter lifetime (Schweitzer-Stenner et al., 1992a,b; Erickson et al., 1991). As a consequence, their capability to initiate release is rather limited.

(ii) The D_{lh} and D_{hh} produced by the three mAbs do not differ significantly in terms of thee parameters determining the stimulation of the RBL cells. In line with what one expects, the releasable β-hexosaminidase fraction f_R of the cells has been found to be similar for all mAbs (cf. Table 4). The probability parameter σ_0, which determines the release time course in the initial phase, is practically identical for J17 and F4 and only slightly lower for H10. Thus, differences in the apparent stimulation capacity as reflected by the release curves

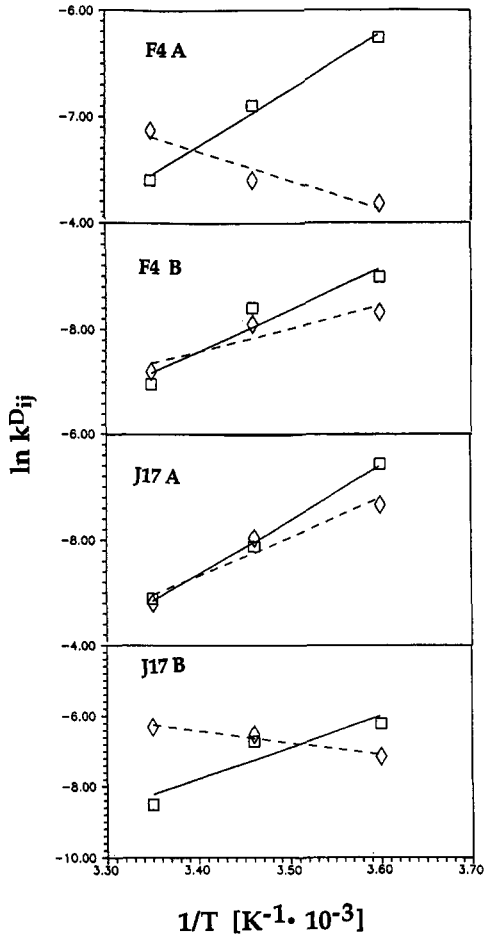

FIGURE 7: Arrhenius plots of the rate constants k^D_{23} (□), k^D_{32} (◇) (A), k^D_{34} (□) and k^D_{43} (◇) (B) derived from the kinetics of F4–FcεRI and J17–FcεRI interaction. The plots were observed for the analysis of the dissociation and association data measured at 25, 15, and 4 °C.

obtained at low mAb concentrations (cf. F4 D, J17 D, and H10 B in Figure 4) are predominantly due to differences in the concentration of the D_{lh} and D_{hh} species produced in the time interval of the measurements.

(iii) The difference in the maximal secretion induced by the mAbs employed can thus be primarily attributed to the desensitization which is also initiated by the FcεRI dimers. It follows directly from eqs 17 and 18 that the mAbs causing the largest dimer formation (H10, J17) are most effective in causing desensitization. This occurs even at intermediate mAb concentrations (10^{-9} M) and lowers the secretion at high mAb concentrations (10^{-8} M). Due to its low dimerization capacity, however, even high concentrations of F4 cause rather limited desensitization, so that the secretory response to this mAb is rather high (i.e., the maximal molar fraction of dimers is between 20 and 30%; Ortega et al., 1988).

Taken together, analysis of the kinetics of mAb–FcεRI interaction and of the corresponding secretory response suggests that the conformational l → h transition within the mAb–$(Fc\varepsilon RI)_2$ complexes produces dimers with lifetimes which are sufficiently long to make them all effective secretagogues. The extent of the cell stimulation is determined by the concentration of the corresponding D_{lh} and D_{hh} species. It is assumed that at high dimer concentrations a desensitization process is initiated which counteracts stimulation, thus reducing the maximal secretion to levels significantly lower than those of the potentially releasable content of the cells (i.e., $f_R = 0.85$).

Several important questions remain unanswered. First, the nature of underlying biochemical processes causing the desensitization initiated by FcεRI clusters is unknown. Second, the nature of the FcεRI conformational equilibria controlled by ligand binding requires structural studies. Third, it will be necessary to explore the temporal relationships between the coupling processes, e.g., the influx of extracellular Ca^{2+} (Beaven et al., 1984), the phosphorylation–dephosphorylation of specific proteins (Pecht et al., 1991a; Choi et al., 1994), and the production of inositol phosphates with the extent of FcεRI dimerization (Pecht et al., 1991a).

Activation Barriers of the Dimerization Process. The rate constants of the mAb–FcεRI interactions can be classified on the basis of their temperature dependence as follows: (1) The rate constants of dimer formation k^D_{12} were found to be practically temperature independent. This suggests that the activation barrier is predominantly of an entropic nature, in full accordance with the considerations presented below. (2) Surprisingly the rate constants k^D_{23}, k^D_{34}, and k^D_{43} decrease with increasing temperature. The very same behavior has been observed for k^M_{23} (Ortega et al., 1991). Only the reverse rate constant k^D_{32} ($D_{lh} \rightarrow D_{hh}$) (and correspondingly k^M_{32}) exhibits a regular behavior in that it increases with rising temperature. The activation enthalpies of all reaction steps involved in the dimer formation process were derived from Arrhenius plots of the respective rate constants:

$$\ln k^D_{ij} = \ln A^D_{ij} - H^D_{ij}/KT \qquad (20)$$

where A^D_{ij} and H^D_{ij} ($i, j = 1, 2, 3, 4$) are the preexponential factor and the activation enthalpy of the transition from state i to state j of reaction 1. The preexponential factor A^D_{ij} can be written as

$$A^D_{ij} = \ln v^D_{ij} + S^D_{jj}/R + 1 \qquad (21)$$

where v^D_{ij} is a frequency factor specific for each reaction step and S^{μ}_{ij} is the entropic contribution to the activation barrier of the reaction $i \rightarrow j$. The Arrhenius plots are shown in Figure 7. From the fitting of eq 20 one calculates the activation enthalpy and the preexponential factor for each rate constant as listed in Table 3.

The negative activation enthalpies found for the transitions $D_{ll} \rightarrow D_{lh}$, $D_{lh} \rightarrow D_{hh}$, and $D_{hh} \rightarrow D_{lh}$ indicate that the Arrhenius model is inappropriate for describing these processes and that apparently the activation barriers are themselves temperature dependent. We assume that the FcεRI dimers are affected by FcεRI interactions with membranal and cytosolic components. This is in agreement with results of experiments where we investigated the FcεRI patch formation caused by (tetramethylrhodamine) labeled mAb binding at different times (30, 60, 180 min) and temperatures [25 and 4 °C by use of a fluorescence microscope (cf. Kubitscheck et al. (1991)]: Whereas no patches were observed at 4 °C during the above times by any of the mAbs employed, at 25 °C J17 and F4 gave rise to considerable patch formation within 1 h, while H10 failed to cause it. Patch formation could be partially abrogated by adding a large excess of unlabeled IgE. A fraction of approximately 10% of these patches remained, however, unaffected even after 2 h of IgE incubation (Kircheis et al., unpublished results). These results seem to indicate that the FcεRI dimers formed by J17 and F4 binding are stabilized at higher temperatures in line with the kinetic data. In general, the above fluorescence measurements show that such FcεRI oligomers, being capable of activating RBL cells, undergo further clustering, most probably by interaction with mem-

branal and/or cytosolic components (Menon et al., 1984). Indeed evidence has been provided by fluorescence bleaching recovery experiments (Menon et al., 1986) that such interactions lead to rapid immobilization of the $Fc_\epsilon RI$ complexes within some seconds. The subsequent formation of visible patches seems to be a consequence of this process. Such an immobilization of the $Fc_\epsilon RI$ has recently been shown to occur upon their dimerization by F4 and J17 to a degree that correlates with their capacity to cause a secretory response (Pecht et al., 1991b).

As shown above, the rate constants of the l → h and h → l transitions induced in J17 and F4 dimers at 4 °C are consistent with those obtained for the corresponding monomeric complex. At 25 °C, however, these D_{hh} complexes dissociate much slower than expected from the above results. This is indicative of some stabilizing interactions not operative at 4 °C.

The Probability of Dimer Formation Is Enhanced in the Two Dimensions on the Cell Membrane. Earlier studies have shown that the equilibrium constant for a process whereby two independent binding sites are cross-linked by a divalent ligand should be equal to or smaller than half the association constant describing the intrinsic binding of this ligand to one binding site (Dembo & Goldstein, 1978a,b; Schweitzer-Stenner et al., 1987). This means in the present case that $K^D \leq K^M/2$. The dimer formation constant derived from our binding and kinetic data are, however, considerably larger than the corresponding intrinsic binding constant of the reaction (cf. Table 2). Inspection of the rate constants shows that this is due to the higher association rate constants k^D_{12}. Similar observations were made in studies of the cross-linking of $Fc_\epsilon RI$-bound anti-dinitrophenyl IgE mAbs by bivalent haptens (Erickson et al., 1991). This observation can be rationalized by the theory developed by Grasberger et al. (1985) for membrane receptor clustering. They argued that macromolecular aggregation in solution usually proceeds in the high-dilution limit, where the reactant concentration equals its activity. In this case, one would expect that the above relation between intrinsic binding and dimer formation constants is valid. This is indeed in agreement with recently obtained results for the interactions between divalent haptens and IgE class antibodies in solution (Schweitzer-Stenner et al., 1987, 1992a,b). The situation is different, however, when the reaction takes place on a two-dimensional surface densely occupied by the reactants. In this case the equilibrium constant reflecting the intrinsic interaction free energy of the reactants on the cell's surface can only be obtained when the mass-action law is formulated in terms of their activities. In order to describe the dimerization process in terms of concentrations expressed in molar units, the present theory instead makes use of an apparent equilibrium binding constant K^D, which is the following:

$$K^D = \Gamma_{cor} K^D{}_0 \tag{22}$$

where $K^D{}_0$ is the value of the equilibrium constant measured at the high-dilution limit (i.e., only a small fraction of the surface is occupied with receptors). The correction factor Γ_{cor} can be written as the product

$$\Gamma_{cor} = \Gamma_{trans}\Gamma_{rot}\Gamma_{exc} \tag{23}$$

which accounts for the restrictions in translational (Γ_{trans}) and rotational mobility (Γ_{rot}) and the effect of volume exclusion of the membrane resident receptors (Γ_{exc}) (Grasberger et al., 1985; Minton, 1989) compared with the situation in an isotropic and dilute solution. In order to estimate the possible contributions of these effects to the $Fc_\epsilon RI$ dimerization process, we utilized the expressions developed by Grasberger et al. (1985). These yield a correction factor of $\Gamma_{cor} = 1.3 \times 10^6$, which is considerable and demonstrate the marked enhancement expected for $Fc_\epsilon RI$ dimerization by translational and rotational constraints. This contribution to the free energy change caused by the dimerization process is purely entropic. Consequently, one expects that $S^D{}_{12} \gg H^D{}_{12}$ and according to eqs 20 and 27 a nearly temperature independent $k^D{}_{12}$. This indeed is in agreement with our results (Table 1).

One further interesting insight can be obtained by comparing the K^D values of the three mAbs measured at 25 °C. These values reflect differences in the corresponding intrinsic binding constant K^M [note that K^D is proportional to K^M (Dembo & Goldstein, 1978b)] and/or in the correction factor Γ_{rot}. Since Γ_{exc} and Γ_{trans} do not depend on the choice of the cross-linking agent, the ratio K^D/K^M should depend on Γ_{rot} only. This in turn is determined by the maximal tilt angle of a cone in which the main axis of the monomeric mAb–$Fc_\epsilon RI$ complex is allowed to rotate freely around the normal to the membrane surface. The larger this tilt angle, the smaller is Γ_{rot}. Taking the corresponding values from Table 2, one obtains the K^D/K^M ratio of 56 for F4, 166 for J17, and 4500 for H10. This suggests that $\Gamma_{rot}(H10) > \Gamma_{rot}(J17) > \Gamma_{rot}(F4)$, indicating that the orientational constraints imposed on the $Fc_\epsilon RI$–mAb complexes increase (i.e., the maximal tilt angle decreases) in the order $Fc_\epsilon RI$–F4, $Fc_\epsilon RI$–J17, and $Fc_\epsilon RI$–H10. It is interesting to note that this trend correlates with the secretion-inducing capacity of these mAbs (Ortega et al., 1988).

APPENDIX: SEMINUMERICAL SOLUTION OF EQ 6

In order to solve eq 6 seminumerically, we first treat all rate equations separately. They can be written as

$$dL_m(t)/dt = \theta_m(t) + c_m(t)\, L_m(t) \tag{A1}$$

where L_m ($m = 1, 2, ..., 9$) is a component of the vector defined by eq 6. Each $L_m(t)$ corresponds to a function $\phi_m(t)$ which depends on the variables L_1, ..., L_9. The coefficient $c_m(t)$ is a function of $[Fc]_f$ for L_1, ..., L_5, L_7, and L_8 and a constant for the remaining m values. To a first approximation we also regard ϕ_m and c_m as constants. Thus the solution of eq A1 is given by

$$L_m(t) = (L_{m0} + \phi_m)\exp(-c_m t) - \phi_m \tag{A2}$$

where L_{m0} denotes the initial concentration of species L_m.

In the numerical procedure employed we subdivided the time period of the experiment into $n = 1000$ time intervals δt. For each of these intervals we first calculated the concentrations $L_{m,i}$ present at $t_i = i\delta t$ ($i = 1, 2, ..., n$) assuming that for each $L_{m,i}$ the concentrations of the other species do not change in the interval δt. Hence, as a first guess $L_{m,i,j=1}$ were expressed by

$$L_{m,i,j=1} = \{L_{m,i-1} + \phi_{m,i-1}\}\exp(-c_{m,i-1}\delta t) - \phi_{m,i-1} \tag{A3}$$

The parameters $\phi_{m,i-1}$ and $c_{m,i-1}$ depend on the concentrations $L_{m,i-1}$ present at t_{i-1}. In the second step the thus obtained $L_{m,i,j=1}$ were used to calculate new values for the parameters ϕ_m and c_m, which we now denote as $\phi_{m,i,j=1}$ and $c_{m,i,j=1}$. They were then employed to calculate $L_{m,i,j=2}$. This was repeated until convergence was reached, i.e., $|L_{m,i,j} - L_{m,i,j-1}| < 0.001 L_{m,i,j}$. This procedure was carried out for all t_i to obtain the time dependence of $L_m(t)$.

ACKNOWLEDGMENT

We would like to thank Dr. Ulrich Pilatus and Dipl. Phys. Martin Kircheis for valuable discussions and for critically reading the manuscript.

REFERENCES

Balakrishnan, K., Hsu, T. J., Cooper, A. D., & McConnell, H. M. (1982) *J. Biol. Chem. 257*, 6427–6433.

Barsumiann, E. L., Isersky, C., Petrino, M. G., & Siraganian, R. (1981) *Eur. J. Immunol. 11*, 317–323.

Beaven, M. A., Rodger, J., Moore, J. P., Hesketh, T. R., Smith, G. A., & Metcalfe, J. D. (1984) *J. Biol. Chem. 259*, 7129–7136.

Braunstein, D., & Spuddich, A. (1994) *Biophys. J. 66*, 1717–1725.

Choi, O. H., Adelstein, R. S., & Beaven, M. A. (1994) *J. Biol. Chem. 269*, 536–541.

DeLisi, C. (1980) *Q. Rev. Biophys. 13*, 201–230.

DeLisi, C. (1981) *Nature (London) 289*, 322–323.

DeLisi, C., & Siraganian, R. P. (1979) *J. Immunol. 122*, 2293–2299.

Dembo, M., & Goldstein, B. (1978a) *Immunochemistry 15*, 307–313.

Dembo, M., & Goldstein, B. (1978b) *J. Immunol. 121*, 345–353.

Dembo, M., Goldstein, B., Sobotka, A. K., & Lichtenstein, L. M. (1979) *J. Immunol. 123*, 1864–1872.

Dower, S. K., DeLisi, C., Titus, J. A., & Segal, D. M. (1981) *Biochemistry 20*, 6326–6334.

Erickson, J. W., Kane, P., Goldstein, B., Holowka, D., & Baird, B. (1986) *Mol. Immunol. 72*, 769–781.

Erickson, J. W., Posner, R. G., Goldstein, B., Holowka, D., & Baird, B. (1991) *Biochemistry 30*, 2357–2363.

Eshhar, Z. (1985) in *Hybridoma Technology in the Biosciences and Medicine* (Springer, T., Ed.) pp 3–40, Plenum, New York.

Goldstein, B., Dembo, M., & Malveaux, F. J. (1979) *J. Immunol. 122*, 830–833.

Grasberger, B., Minton, A. P., DeLisi, C., & Metzger, H. (1985) *Proc. Natl. Acad. Sci. U.S.A. 83*, 6825–6262.

James, F., & Ross, M. (1975) *Comput. Phys. Commun. 10*, 343–354.

Kagey-Sobotka, A., Dembo, M., Goldstein, B., Metzger, H., & Lichtenstein, L. M. (1981) *J. Immunol. 127*, 2285–2291.

Kane, P., Erickson, J. W., Fewtrell, C., Baird, B., & Holowka, D. (1986) *Mol. Immunol. 23*, 783–790.

Kane, P., Holowka, D., & Baird, B. (1988) *J. Cell Biol. 107*, 969–980.

Kinet, J. P., & Metzger, H. (1990) in *Fc receptors and the action of antibodies* (Metzger, H., Ed.) p 239, American Society of Microciology, Washington, DC.

Kubitscheck, U., Kircheis, M., Schweitzer-Stenner, R., Dreybrodt, W., Jovin, T. M., & Pecht, I. (1991) *Biophys. J. 60*, 307–318.

Kubitscheck, U., Schweitzer-Stenner, R., Arndt-Jovin, D., Jovin, T. M., & Pecht, I. (1993) *Biophys. J. 64*, 110–120.

Menon, A. K., Holowka, D., & Baird, B. (1984) *J. Cell Biol. 98*, 577–583.

Menon, A. K., Holowka, D., Webb, W. W., & Baird, B. (1986) *J. Cell Biol. 1986*, 541–550.

Minton, A. L. (1989) *Biophys. J. 55*, 805–808.

Oliver, J. K., Seagrave, J. C., Stump, R. F., Pfeiffer, J. R. & Deanin, G. G. (1988) *Prog. Allergy 42*, 185–245.

Ortega, E., Schweitzer-Stenner, R., & Pecht, I. (1988) *EMBO J. 7*, 4101–4109.

Ortega, E., Schweitzer-Stenner, R., & Pecht, I. (1991) *Biochemistry 30*, 3473–3483.

Pecht, I., Schweitzer-Stenner, R., & Ortega, E. (1989) *Prog. Immunol. 7*, 676–682.

Pecht, I., Ortega, E., & Schweitzer-Stenner, R. (1991a) in *Biological Signal Transduction* (Ross, E. M., & Wirtz, K. W. A., Eds.), pp 147–162, Springer, Heidelberg.

Pecht, I., Ortega, E., & Jovin, T. M. (1991b) *Biochemistry 30*, 345–3458.

Posner, R. G., Erickson, J. W., Holowka, D., Baird, B., & Goldstein, B. (1991) *Biochemistry 30*, 2348–2356.

Reck, B., Sagi-Eisenberg, R., & Pecht, I. (1985) *Proceedings of the XII International Congress of Allergology and Clinical Immunology*, pp 164–169, Mosby Company.

Rudolph, A. K., Burrows, P. D., & Wahl, M. R. (1981) *Eur. J. Immunol. 11*, 527–529.

Schweitzer-Stenner, R., Licht, A., Lüscher, I., & Pecht, I. (1987) *Biochemistry 26*, 3602–3612.

Schweitzer-Stenner, R., Licht, A., & Pecht, I. (1992a) *Biophys. J. 63*, 551–562.

Schweitzer-Stenner, R., Licht, A., & Pecht, I. (1992b) *Biophys. J. 63*, 563–568.

Sperotto, M. M., & Mouritsen, O. G. (1991) *Eur. Biophys. J. 19*, 157–168.

Weiss, R. M., Balakrishnan, K., Smith, B. A., & McConnell, H. M. (1982) *J. Biol. Chem. 257*, 6440–6445.